International Micro Air Vehicle Conference and Flight Competition (IMAV2013)
17-20 September 2013, Toulouse, France

# Aerodynamic Characteristics of a Low Aspect Ratio Wing and Propeller Interaction for a Tilt-Body MAV

Kwanchai Chinwicharnam[1]*, David Gomez Ariza[2]†, Jean-Marc Moschetta[2]‡ and Chinnapat Thipyopas[1]§

[1] Kasetsart University, Bangkok, Thailand
Chinwicharnam.Kwarchai@isae.fr
[2] Institut Supérieur de l'Aéronautique et de l'Espace, Toulouse, France
Jean-Marc.Moschetta@isae.fr

**Abstract**

An experimental investigation of the interaction of a propeller-wing configuration for a tilt body MAV VTOL was performed in the low speed wind tunnel. This study's primary objective is to present the effect of the interaction between a low aspect ratio wing and propeller for the range of incidence in transition between horizontal and vertical flight. During the transition from horizontal flight to vertical flight or vice versa, the flow patterns seen by the wing are the result of the combination between the free-stream and the propeller flow. This was reflected in the change of the aerodynamic forces and moments of the wing. The model is a tractor configuration which is a Graupner propeller and wing with aspect ratio 1, an airfoil NACA 0012. All tests were conducted at low speeds in a range from 2 to 8 m/s. In order to simulate the transition flight of a MAV VTOL a range of incidence from -10 to 90 degree was used. The results show that the flow patterns of the propeller certainly improve the aerodynamic characteristics of the wing, increase lift and delay stall angle with respect to the flight path of the MAV.

## 1 Introduction

The interaction between wing and propeller was considered for improving the aerodynamic performance of MAV. The propeller propulsive system, which is the main power for flight operation, is a problem of MAV aerodynamic because the motor and propeller are located across the free stream; and correspondingly the propeller generates slipstream. The position of propeller influence on the wing boundary layer characteristics such as: laminar flow extension and transition, laminar separation bubbles, and reattachment and turbulent separation. This has been found and compared the different between tractor and pusher configuration by Catalano[1] which states that pusher propeller inflow affects the wing characteristics by changing the lift, drag, and also the boundary layer transition and separation point. The propeller slipstream is a cause of variable flow property around surface of MAV and induces the free stream velocity for MAV. To understand the behavior of the flow seen by the wing, the experiment was organized in order to analyze the difference between the isolated wing and the mounted propeller-wing. The effect of propeller wash or slipstream on the wing aerodynamic during transition flight was the focus and the fixed-wing tractor configuration was considered.

*Master student of Kasetsart University
†PhD. student of ISAE (davinciig@yahoo.com)
‡Professor, Institut Supérieur de l'Aéronautique et de l'Espace, Toulouse, France.
§Advisor, Department of Aerospace Engineering, Kasetsart University, Bangkok, Thailand. (fengcpt@ku.ac.th)

Similar researches has shown that the slipstream effect to the stall delay, lift augmentation, drag increase, and reduced aerodynamic efficiency [2][3]. This research studied and supported the Mini-Vertigo MAV configuration was a co-axial propeller. Maxime [4] studied the characteristic longitudinal flight behavior during an equilibrium transition between vertical/horizontal flight modes and were investigated for enhancement of the longitudinal control of the MAVion (a tractor configuration MAV of ISAE). This test found the interaction wing and propeller and the model has 2 propellers. Deng et al.[5] studied the propeller-wing interaction both the experiment and numerical method. It was found that the slipstream has a significant influence on the pressure distribution on the wing surface, as well as, explained the pattern of wing-tip vortex in different of the angle of attack with rotary propeller. However, the test is limited at low angle of attack. Therefore, the aerodynamic part of interaction wing and propeller is essential to study and understand the performance of MAV during trasition flight, especially. Moreover, the wing wash effect which several researches neglected has been considered in this paper. This current research investigates the effect of propeller-wing interaction in a tractor configuration by performing an experiment. A three dimensional NACA 0012 rectangular wing and Grauper Super Nylon propeller was performed in the Supaero low speed wing tunnel (SabRe). The isolated wing and propeller were conducted and then the mounted propeller-wing was considered at the same condition.

## 2 Test Subject

The model in this study is a tractor configuration. The detail of model is in Figure 1. The test was achieved at ISAE by the SabRe wind-tunnel. The model was investigated both at a low incident angle and high incident angle; thus the range of angle of attack varies from -10 to 90 degrees. The model was also designed with a plain flap in order to study the flap deflection effect. In this experiment was focused at the low Reynolds Number(Re) . Moreover, the installations propeller position was also studied in this research.

| Information | Value |
|---|---|
| Airfoil | NACA 0012 |
| Wingspan | 0.3 m |
| Wingchord | 0.3 m |
| Planform shape | Rectangular |
| Wing area | 0.09 $m^2$ |
| AR | 1 |
| Flap type | Plain flap |
| Flap area | 0.03 m |
| Wing material | SLS Materials |
| Motor | Brushless PJS 3D 550 |
| Propeller | Graupner 8x6" |
| Motor support | Aluminum |

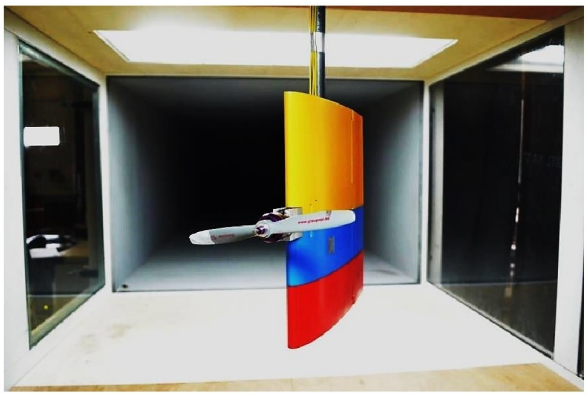

Figure 1: Model information and tractor configuration model in SabRe

## 3 Experimental Setup

The experiment was performed using four different models: a singular propeller model was achieved by David[6], a wing alone model, MPROWM (Mounted propeller on wing model) and SPROWM (Separated propeller on wing model). The model was installed in the closed-circuit low speed wind tunnel of ISAE (SabRe) with test section 1.2m x 0.8m and 2.4m long.

The model was positioned vertically. The propeller was moved by the aluminum motor support wedges. The propeller (l) was set in position at 7%c and 18%c ahead of wing leading edge(LE). The model was turned from -10 to 90 degree by the using an automatic rotated motor, in order to measure the angle of attack effect of the models. The flap deflections, in a range from -10 to +20 degrees, were moved by a digital servo mechanism inside the wing. The propeller speeds were fixed at 5,000 RPM. The free stream velocity was set in a range from 2 to 8 m/s.

The isolated wing, MPROWM and SPROWM were carried out in the SabRe wind tunnel shown in Figure 2(a) and 2(b). The forces and moments were measured by the internal five-component Micro Sting Balance aerodynamic which limited at 10 N forces and 0.5 N-m moments. It was made of high strength 35NCD16 alloy steel which calibrated by Thipyopas [7]. All connectors were connected to the National Instrument; PXI-6281 and PXI-6229 card were used to measure the voltage-usage for balance and current-usage for rotational propeller, respectively. Data was collected through the Labview program at 1,000 Hz and recorded every 10 second. Moveover, there are 10 samples for each AOA were used in order to get the accurate data. Note: all of data has been corrected through the wind tunnel wall effects, which is the method of Pope [8].

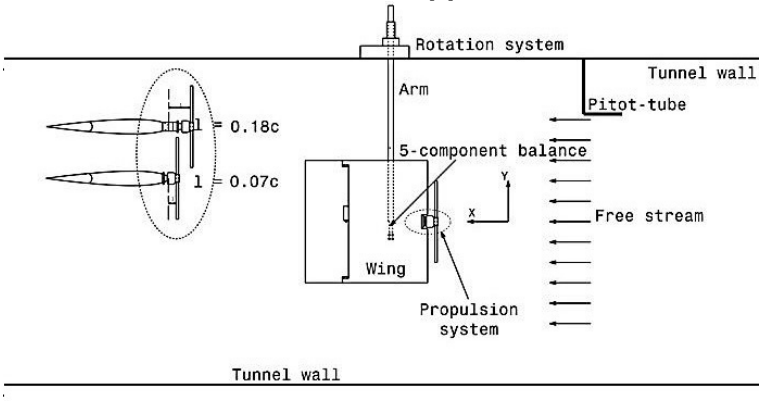


(a)

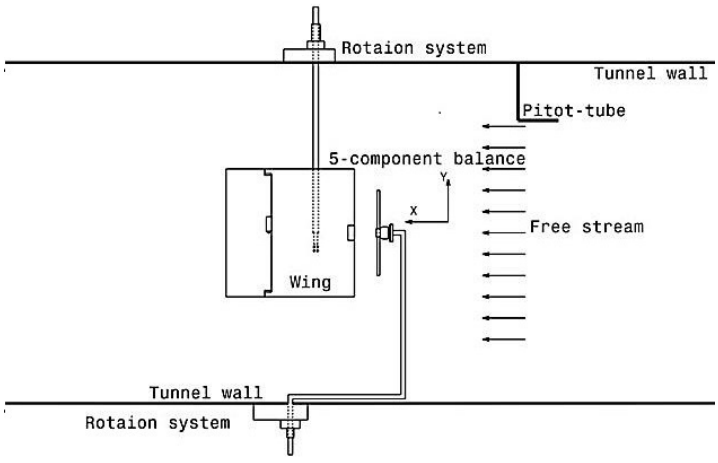


(b)

Figure 2: a) Wind-tunnel tests set up of MPROWM, b) Wind-tunnel tests set up SPROWM

# 4 Results

The aerodynamic coefficient in this paper can be calculated as:

$$C_L = \frac{L}{\frac{1}{2}\rho V^2 S},\ C_D = \frac{D}{\frac{1}{2}\rho V^2 S},\ C_M = \frac{M}{\frac{1}{2}\rho V^2 Sc},\ C_X = \frac{X}{\frac{1}{2}\rho V^2 S}$$

## 4.1 Mounted Propeller on Wing Model (MPROWM)

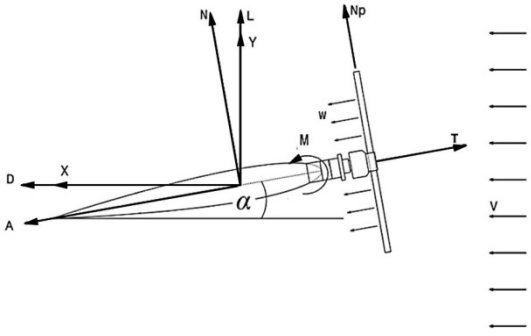


Figure 3: Free body diagram of MPROWM

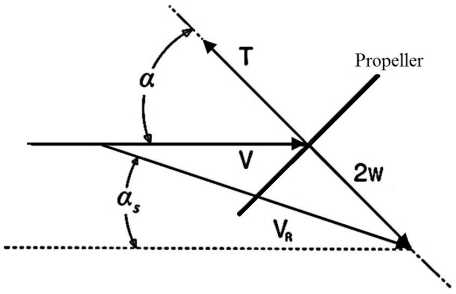


Figure 4: Velocity triangle of fully accelerated slipstream

The balance was set inside the wing and then it was calibrated forces and moments by the standard weight. The AOA and flap deflection angle was calibrated as well. The error is very small and can be ignored. The propeller was mounted with the wing at 7%c ahead of the wing LE. The test fixed the rotating speed at 5000 RPM. The force vector is considered in terms of free body diagram in Figure 3. In the combination of wing-propeller as the MPROWM; the resulting aerodynamic forces are generated by the combination of the singular propeller forces, the single wing forces, and the effect of the propeller wash over the wing. The main effect of the propeller wash over the wing can be seen by the changing effect of AOA on the wing. This AOA can be calculated by using the method in suggested by McCormick[9] that the propeller can make the induced velocity ahead of the wing as shown the velocity triangle of fully accelerated slipstream in Figure 4. In Figure 5(a) shows the ratio of the induced velocity for the general case to the induced velocity in hover case increases with the increment of AOA. And a cause of the effective wing angle of attack ($AOA_w$) is the slipstream resulting velocity ($V_R$) which is the combination between the forward velocity and induced velocity. The evolution of $AOA_w$ as a function of the MPROWM AOA is plotted for V= 8 m/s in Figure 5(b) and the estimation of wing AOA is simply equal to:

$$AOA_w = AOA - AOA_{slipstream} \tag{1}$$

## 4.2 Wing and Propeller Wash Effect

### 4.2.1 Lift Coefficient

In Figure 6(a), the variation of wing prop-on (MPROWM) and wing alone lift with AOA are compared. The figures show the propeller slipstream has a strong stall-delay effect and they have the perfect linear

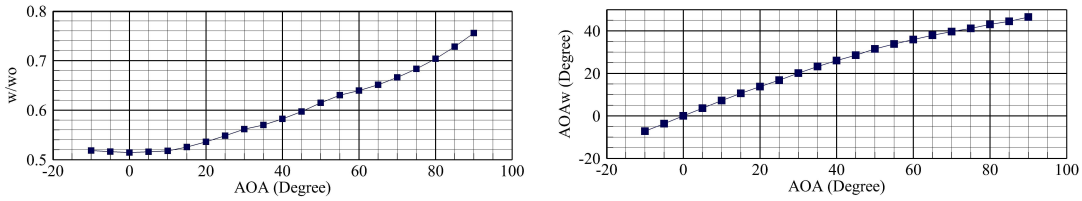


(a) (b)

Figure 5: Propeller slipstream effect when V=8m/s RPM5000: (a) induced velocity, (b) wing angle of attack

slope at post-stall. The stall angle moves from 25 degrees to 40 degrees, as well as, the maximum wing prop-on lift increases by 130%. Consider the generated lift coefficient in each part of MPROWM, which can be derived as:

$$C_{Lwing-prop} = C_{Lwing} + C_{Lprop} + \triangle C_{Lwing/prop} + \triangle C_{Lprop/wing} \tag{2}$$

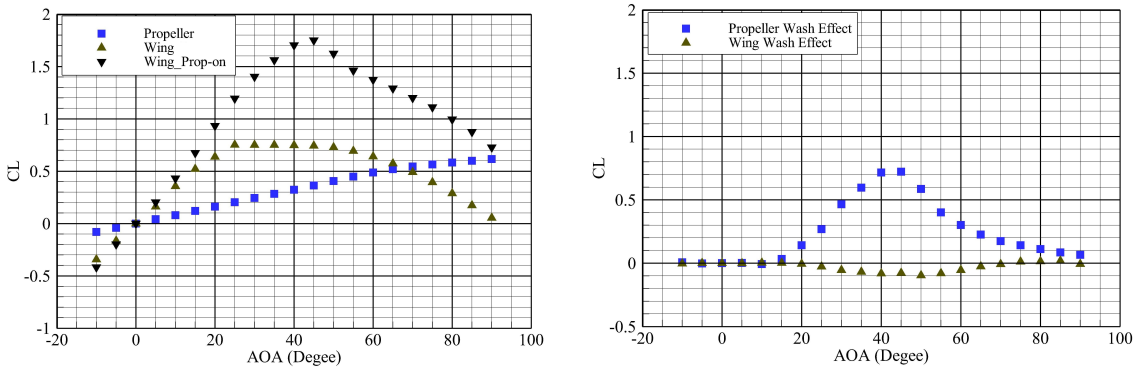


(a) (b)

Figure 6: (a) Propeller, Wing and MPROWM lift coefficient versus angle of attack, (b) Propeller/Wing wash effect lift coefficient versus angle of attack : when V = 8 m/s RPM 5000

Consider the stall angle of the wing prop-on is at 40 degrees, but the true wing AOA is 25 degrees from Figure 6(b) that is also the stall angle of the wing prop-off. This proves Equation 1 works. Notice the including lift coefficient of wing prop-off and on is less than MPROWM lift coefficient. This shows that something promotes the wing and propeller interaction effect. Hence the SPROWM was performed and investigated the propeller wash effect and wing wash effect shown in Figure 6(b). It seems the MPROWM gains lift from wing and propeller only at -10 to 15 degrees. Subsequently, the propeller slipstream has a strong effect on the model up to its maximum of 40-45 degrees, which is the stall angle. These results confirm again that the propeller slipstream can develop the wing boundary layer characteristics such as: laminar separation bubbles, reattachment and turbulent separation; as the suggestion by Catalano [1]. A cause of the stall delay is supposed that the flow reattaches to the wing surface again due to the propeller slipstream (Propeller-wash effect) $\triangle C_{Lwing/prop}$. Therefore the propeller wash effect has been connected to the cause of the MPROWM lift generated. However the wing wash effect $\triangle C_{Lprop/wing}$ which is resistant to the MPROWM lift has also been observed.

It is small effect to propeller, the maximum is about 14% of Max. $\triangle C_{Lwing/prop}$ at stall angle, and negative value during stall of MPROWM as well.

### 4.2.2 Total Longitudinal Force Coefficient

In Figure 7(a) shows $C_X$ wing alone increases continuously with AOA, until the propeller is on. The maximum $C_X$ is still at 90 degrees and rise 13% as a result of the slipstream. In the beginning (-10 to 15 degrees), the offset of wing prop-on and wing alone $C_X$ are completely influenced by the propeller. After this the value of MPROWM $C_X$ is larger than the propeller $C_X$ minus wing prop-off $C_X$. Again the negative value of $C_X$ is with respect to the forward flight direction. Therefore, consider the results generated by $C_X$ in each part of MPROWM.

$$C_{Xwing-prop} = C_{Xwing} + C_{Xprop} + \triangle C_{Xwing/prop} + \triangle C_{Xprop/wing} \tag{3}$$

In Figure 7(b) shows that neither the propeller wash nor wing wash effect at -10 to 25 degrees. Such is the reason of MPROWM $C_X$ value is equal wing prop-off $C_X$ plus propeller $C_X$. Then, the propeller-wash effect $C_X$ increases, which identifies the slipstream as making the incremental increase of MPROWM $C_X$. Hence, the propeller slipstream (Propeller wash effect) prompts the drag for the wing which indicates a concave-up parabolic measurement in the pre-stall and concave-down after the stall. However, after stall angle is found, the result is the wing-wash effect $C_X$. It promotes the reducing of MPROWM $C_X$.

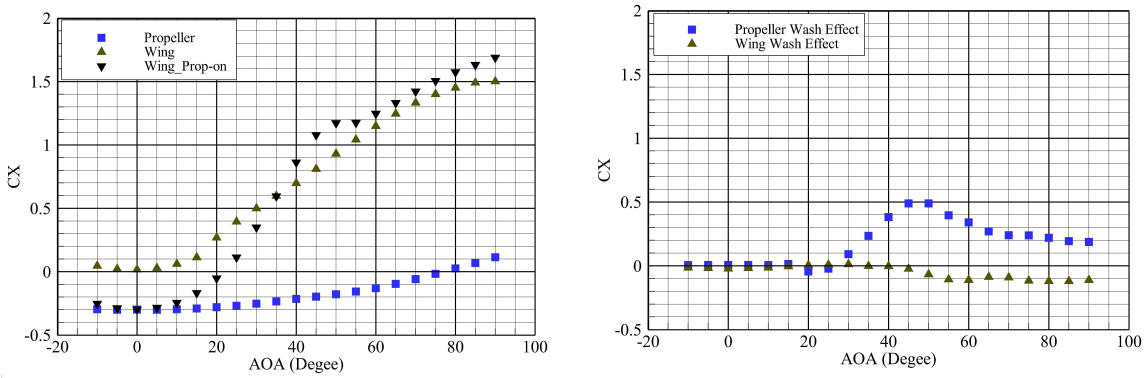


(a) (b)

Figure 7: (a) Propeller, Wing and MPROWM total longitudinal force coefficient versus angle of attack, (b) Propeller/Wing wash effect longitudinal force coefficient versus angle of attack : when V = 8 m/s RPM 5000

### 4.2.3 Pitching Moment Coefficient (LE)

Pitching moment is considered at LE, thus the negative is pitching down and positive is pitching up. In Figure 8(a), the maximum $C_{m(LE)}$ rises 150% due to propeller. The propeller slipstream has still effect to the wing pitching moment. In Figure 8(b) shows that the slipstream has been affected since 15 degrees. It seems the wing can generate more lift by propeller slipstream, thus the MPROWM has more pitching down automatically. The curve of propeller slipstream (Propeller wash effect) is concave-down parabolic measurement in the pre-stall and concave-up after the stall. For the wing wash effect decreases gradually after 15 degrees. It seems the propeller wash and wing wash have an effect to MPROWM $C_{m(LE)}$. Again the MPROWM $C_{m(LE)}$ can be separated for each part as:

$$C_{m(wing-prop)} = C_{m(wing)} + C_{m(prop)} + \triangle C_{m(wing/prop)} + \triangle C_{m(prop/wing)} \quad (4)$$

where $C_{m(prop)} = C_T \cdot r + C_{Np} \cdot l$. The average $C_T$ is close to the propeller center $(r)$, but to $r$ is very small. Thus $C_T \cdot r$ is considered to be zero. $l$ is the propeller position from the wing LE.

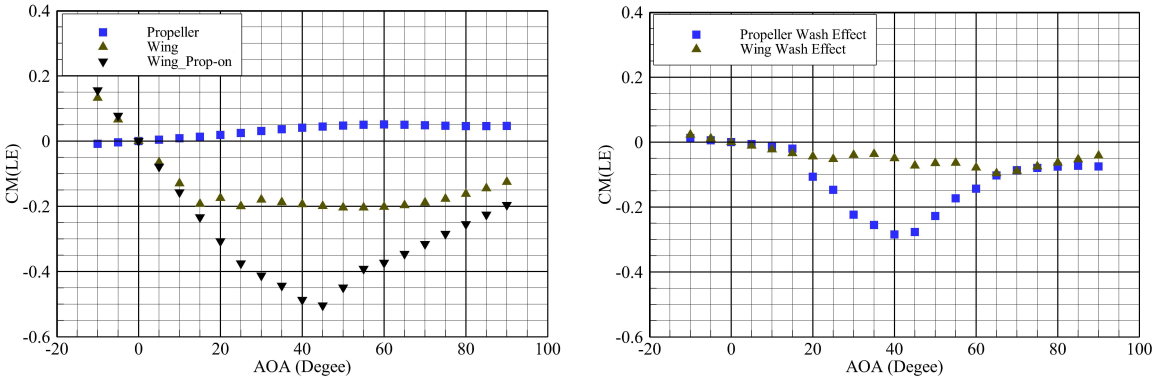


(a) (b)

Figure 8: (a) Propeller, Wing and MPROWM pitching moment coefficient versus angle of attack, (b) Propeller/Wing wash effect pitching moment coefficient versus angle of attack : when V = 8 m/s RPM 5000

## 4.3 Streamwise Propeller Position Effect

The position of propeller was changed from 7% to 18% of mean aerodynamic chord ahead of wing LE in order to investigate what effect of the propeller slipstream has on the wing. Figure 9, found that the slope over the stall of the wing for a propeller located at 18%c decreases immediately but the propeller located at 7%c gradually reduces . This seems that the propeller, which is closer to the wing, can control the flow around the wing and improve it. That propeller position may also help the flow attach more to the wing surface. The flow after stall angle improves by propeller-wash; the blue line, which is the influence of propeller wash on the wing, can be explained clearly by the $C_L$,$C_X$ curve are smooth concave-down parabolic.

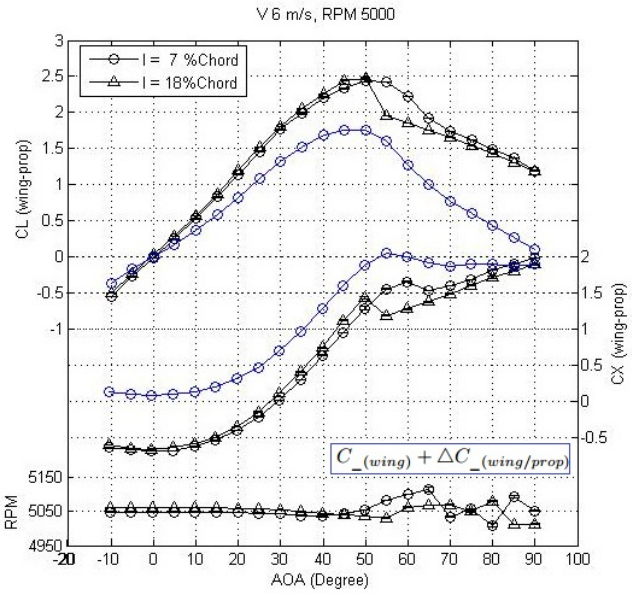


Figure 9: Lift, Drag coefficient and RPM vs AOA

The best performance of the wing is obtained when the propeller is installed close to the wing as the previous studies as the one presented in [10]showed the results at low AOA. Moreover, the current results show that for a high AOA and the results are same case. It should be noted that there are small difference of RPM in each AOA, but there are small energy results which can be ignored.

## 4.4 Flap Deflections Effect

In order to investigate the flap deflections effect, the MPROWM and SPROWM were designed with a flap at -10 to 20 degrees. In above part can see the effect of propeller slipstream takes place on the wing. In Figure 10 shows the influence of propeller slipstream on the wing in terms of variation of flap deflections. The aerodynamic values are improved due to the propeller slipstream develops the boundary layer on the wing surface and keeps laminar flow in higher incident angle. The wing $C_L$ and $C_X$ increase when the flap deflection is positive. Conversely, the wing $C_L$-$C_X$ decrease when the flap deflection is negative. In conclusion, the changing of wing $C_L$ and $C_X$ in each $\pm 10$ degrees of flap deflections are $\pm 0.35$ and $\pm 0.3$ respectively. The flap deflections have no an influence on the wing pitching moment at the leading edge($C_{m,LE}$). We found that the wing lift increases when the flap deploys in positive, and the the pitching moment at 0.3c as well. Therefore, it is normally that the wing pitching moment at LE in variation of flap deflections is not different at post-stall. During the first and second stall angle (20-35 degrees), the curves swing because of the severation flow and the strong turbulent flow on the wing surface. Moveover, the flap of MPROWM is out of control the wing aerodynamic after stall angle because of the slipstream effect.

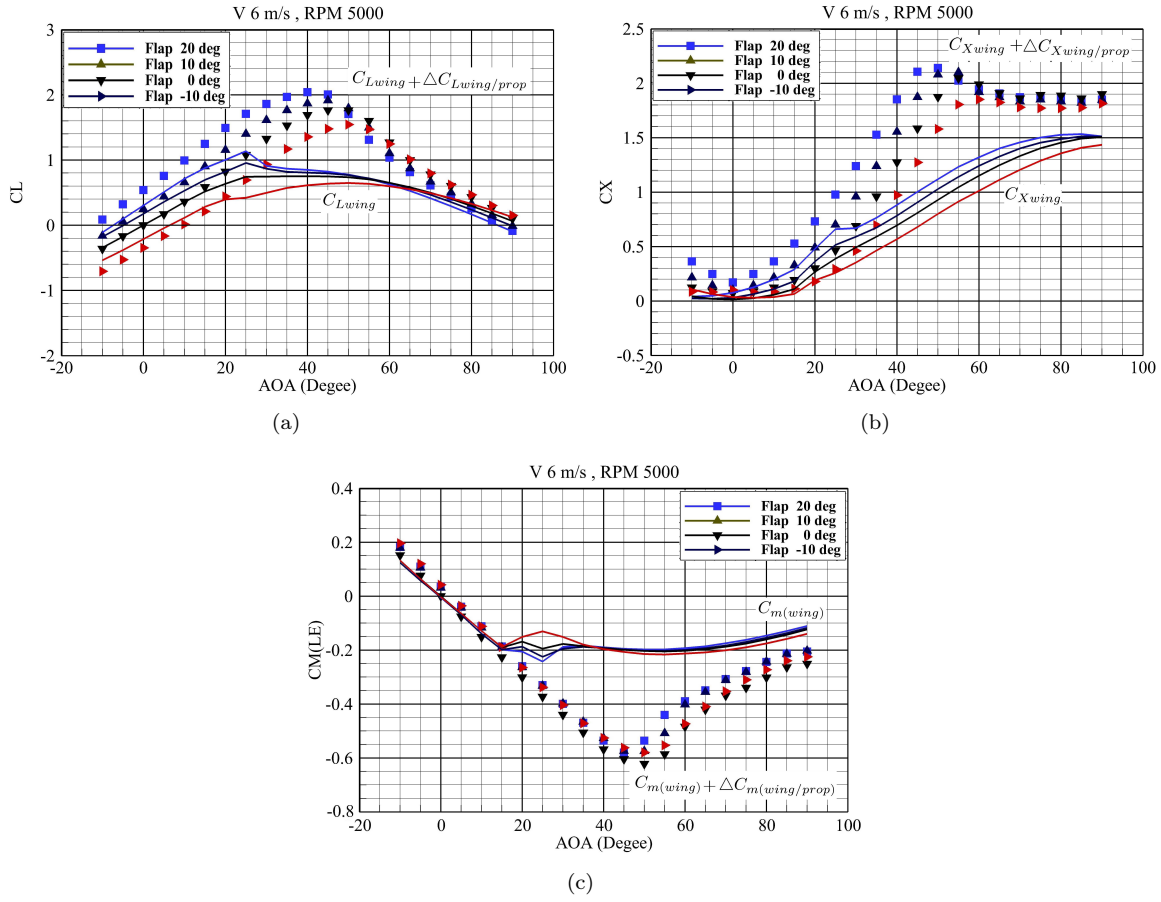


Figure 10: Flap deflection effect on the MPROWM vs AOA: (a) lift coefficient, (b) total longitudinal force coefficient, (c) pitching moment coefficient at leading edge

# 5 Conclusion and Future Work

Due to multi-function of MAVs, it can tilt body from horizontal to vertical flight, as well as hover. Thus it is important to know to aerodynamic characteristics which influence flight control while flying. In order to investigate the aerodynamic characteristics, we focused on the interaction between a wing and propeller. Additionally, this research is different from the other research done with the models. The models of this research are applied by the basic configuration such as: the wing in NACA 0012, the electronic propeller which is general to explain the aerodynamic performance of interaction between wing and propeller for tilt body MAVs. The models were tested in SabRe wind tunnel and found that

- The MPROWM aerodynamic forces and moment are not only generated by the singular wing and propeller, but also the slipstream effect.
- Moreover, the slipstream is divided to propeller-wash effect and wing-wash effect. The propeller-wash has the large effect, but the wing-wash has some small effect to the wing. The influence of propeller-wash on the wing develops the boundary layer and keeps laminar flow in higher incident angle. These effects increase the wing performance and delay stall angle
- The installations with close to the wing are more efficient than those farther. Especially after the wing stall, the wing boundary layer has more the reattach flow, and as well the wing lift has a smooth downward motion.
- Maximum MPROWM lift and drag increases with positive flap deflection and decreases with negative flap deflection at post stall. And slipstream propeller improves the flow around the wing

The experiment data of this study can only explain the interaction between wing and propeller of tilt body MAVs in terms of aerodynamic coefficient. Therefore the future work will use Computational Fluid Dynamic (CFD) methodology. In order to achieve the level of detail to describe the phenomena flow that occurs in the propeller-wing interaction, as well as, confirm the assumption of experimental study about the flow, the numerical methodology uses the FLUENT. This intends to explain the propeller slipstream which is the main point of flow around the wing. The k-$\varepsilon$ RNG turbulent model is applied. The main interest is that the RNG model in FLUENT provides an option to account for the effects of swirl or rotation. The Pressure-Velocity coupling solves to get the convergence by the SIMPLE C algorithm. The propeller is assumed to an actuator disk. Moreover UDF is called for the actuator disk boundary condition which the velocity polynomial profile function of propeller is suggested by Rosen [11]. A structured C-grid type is used and shown in Figure 11(a). The first case at zero AOA has been done and shows the axial velocity contour plot in Figure 11(b), which also found the axial velocity increases at propeller downstream.

# 6 Acknowledgments

The author is indebted and grateful to Chinapat Thipyopas of the Aerospace Engineering of Kasetsart University, Thailand who introduced the research, and Jean-Marc Moschetta of Institut Supèrieur de l'Aèronautiaue et de l'Espace, France who recommended a great deal of this research as well as providing the place and tools for the test. David Gomez Ariza, guided the processing of research and helped solve problems during the test, as well as giving suggestions and exchanges ideas. The author appreciates Rèmi Chanton, Sebastien Prothin and other members of SUPAERO for experimental setup preparation and their involvement. Finally, the author would like to thank Ryan Randall, his previous works helped give invaluable information to this writer.

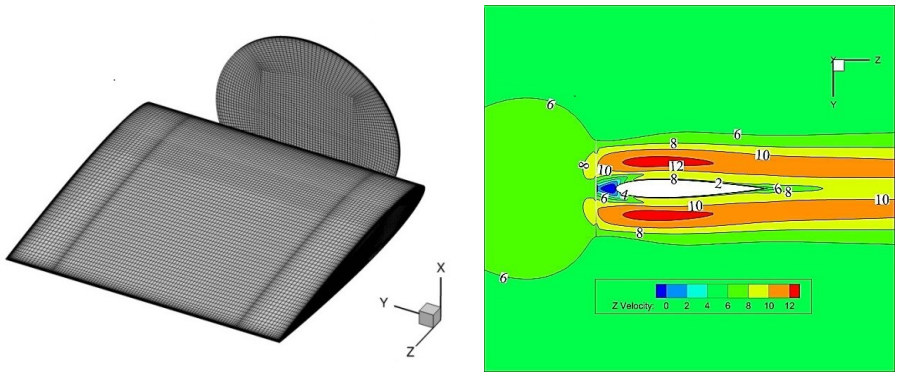


(a) (b)

Figure 11: (a) Structure C-grid of wing and actuator disk, (b) Axial velocity contour plot when the MPROWM AOA 0 degree and freestream velocity 6 m/s

# References

[1] F.M. Catalano. On the effects of an installed propeller slipstream on wing aerodynamic characteristics. *Acta Polytechnica*, 44(3):8–14, 2004.

[2] R. Randall, C.-A. Hoffmann, and S. Shkarayev. Longitudinal aerodynamics of a vertical take off and landing micro air vehicle. *Journal of Aircraft*, 48(1):166–176, January-February 2011.

[3] R. Randall, S. Shkarayev, G. Abate, and B. Judson. Longitudinal aerodynamics of rapidly pitching fixed-wing micro air vehicle. *Journal of Aircraft*, 49(2):453–467, March-April 2012.

[4] M. Itasse, J.-M. Moschetta, Y. Ameho, and R. Carr. Equilibrium transition study for a hybrid mav. *International Journal of Macro Air Vehicles*, 3(4):229–246, November 2011.

[5] S. Deng, B.W. van Oudheusden, T. Xiao, and H. Bijl. A computational study on the aerodynamic influence of a propeller on an mav by unstructured overset grid technique and low mach number reconditioning. *The Open Aerospace Engineering Journal*, 5:11–21, 2012.

[6] D.G. Ariza. *Study of the Sensitivity to the Lateral Wind of a Mini Unmanned Aerial Vehicle with VTOL flight capabilities*. PhD thesis, ISAE, France, 2013.

[7] C. Thipyopas and J.-M. Moschetta. Experimental analysis of a fixed-wing vtol mav in ground effect. *International Journal of Macro Air Vehicles*, 2(1):33–54, March 2010.

[8] A. Pope, J.B. Barlow, and W.H. Rae. *Low-Speed Wind Tunnel Testing*. John Wiley & Sons Inc, New York, 2011.

[9] B. W. McCormick. *Aerodynamics of V/STOL Flight*. Dover, New York, 1967.

[10] V. Leo. *Propeller Wing Aerodynamic Interference*. Delft University of Technology Netherlands, Netherlands, 2005.

[11] A. Rosen and O. Gur. Novel approach to axisymmetric actuator disk modeling. *Journal of AIAA*, 46(11):2914–2925, November 2008.

[12] B. Bataille, J.-M. Moschetta, D. Poinsot, and C. Berard. Development of a vtol mini uav multi-tasking missions. *The aeronautical Journal*, 113(1140):87–98.